Journal of Cleaner Production 430 (2023) 139435

Contents lists available at ScienceDirect

Journal of Cleaner Production

journal homepage: www.elsevier.com/locate/jclepro

Estimation of CO_2 solubility in aqueous solutions of commonly used blended amines: Application to optimised greenhouse gas capture

Farid Amirkhani [a], Amir Dashti [b], Mojtaba Jokar [c], Amir H. Mohammadi [d,e], Abdoulmohammad Gholamzadeh Chofreh [f,g,*], Petar Sabev Varbanov [g], John L. Zhou [b]

[a] Department of Chemical Engineering, Faculty of Engineering, University of Kashan, Kashan, Iran
[b] Centre for Green Technology, School of Civil and Environmental Engineering, University of Technology Sydney, NSW, 2007, Australia
[c] Department of Chemical Engineering and Materials Science, Wayne State University, USA
[d] Institut de Recherche en Génie Chimique et Pétrolier (IRGCP), Paris Cedex, France
[e] Discipline of Chemical Engineering, School of Engineering, University of KwaZulu-Natal, Howard College Campus, King George V Avenue, Durban, 4041, South Africa
[f] Department of Engineering, School of Engineering and the Built Environment, Faculty of Computing, Engineering and the Built Environment, Birmingham City University, B4 7XG, Birmingham, UK
[g] Sustainable Process Integration Laboratory – SPIL, NETME Centre, Faculty of Mechanical Engineering, Brno University of Technology - VUT BRNO, Technická 2896/2, 616 69, Brno, Czech Republic

ARTICLE INFO

Handling Editor: Jin-Kuk Kim

Keywords:
Absorption
Blended amines
CO_2 capture
Data-driven model
Soft computing approach

ABSTRACT

One of the key concerns in the 21st century, alongside the growing population, is the increase in energy consumption and the resulting global warming. The impact of CO_2, a prominent greenhouse gas, has garnered significant attention in the realm of CO_2 capture and gas purification. CO_2 absorption can be enhanced by introducing some additives into the aqueous solution. In this study, the accuracies of some of the most up-to-date computational approaches are investigated. The employed machine learning methods are hybrid-adaptive neuro-fuzzy inference system (Hybrid-ANFIS), particle swarm optimization-adaptive neuro-fuzzy inference system (PSO-ANFIS), least-squares support vector machines (LSSVM) and genetic algorithm-radial basis function (GA-RBF). The developed models were used in estimating the solubility of CO_2 in binary and ternary amines aqueous solutions. i.e. blends of monoethanolamine (MEA), triethanolamine (TEA), aminomethyl propanol (AMP), and methyldiethanolamine (MDEA). This modeling study was undertaken over relatively significant ranges of CO_2 loading (mole of CO_2/mole of solution) as a function of input parameters, which are 0.4–2908 kPa for pressure, 303–393.15 K for temperature, 36.22–68.89 g/mol for apparent molecular weight, and 30–55 wt % for total concentration. In this work, the validity of approaches based on different statistical graphs was investigated, and it was observed that the developed methods, especially the GA-RBF model, are highly accurate in estimating the data of interest. The obtained AARD% values for the developed models are 18.63, 8.25, 12.22, and 7.54 for Hybrid-ANFIS, PSO-ANFIS, LSSVM, and GA-RBF, respectively.

1. Introduction

It is important for our planet to have CO_2 in its atmosphere, while a significant increase in the concentration of this gas can lead to serious effects such as global warming and climate change (Zhang et al., 2023b). For this reason, there has been a lot of interest in new methods for minimising CO_2 emissions to the atmosphere (Li et al., 2023), which can be applied to various industrial plants (Mosadegh et al., 2020).

Absorption (Zhang et al., 2023c), Adsorption (Li, 2023), Cryogenics (Safdarnejad et al., 2015), and Membrane (Amirkhani et al., 2020b) based separation methods are among the methods of reducing CO_2 emissions which have been investigated earlier. The adsorption method has many benefits compared to the other mentioned approaches (Olajire, 2018). There are some disadvantages to activated carbon use, such as low selectivity of CO_2/N_2 (Ben-Mansour et al., 2016). Other adsorbents such as zeolite, alkali metals, amine-based adsorbents, microporous organic polymers, and metal-organic frameworks have also been studied. The adsorption methods for reducing CO_2 emissions in the industry normally require low-temperature conditions for adsorbents

* Corresponding author. Department of Engineering, School of Engineering and the Built Environment, Faculty of Computing, Engineering and the Built Environment, Birmingham City University, B4 7XG, Birmingham, UK.
E-mail address: Authorabdoulmohammad.chofreh@bcu.ac.uk (A. Gholamzadeh Chofreh).

https://doi.org/10.1016/j.jclepro.2023.139435
Received 22 July 2023; Received in revised form 14 October 2023; Accepted 19 October 2023
Available online 31 October 2023

Abbreviations

AARD	Average absolute relative deviation
AI	Artificial intelligence
AMP	Aminomethyl propanol
ANFIS	Hybrid adaptive neuro fuzzy inference system
ANN	Artificial neural network
CCS	Carbon capture and storage
CH_4	Methane
CO_2	Carbon dioxide
CSA	Coupled simulated annealing
DEA	Diethanolamine
EXP	Experimental
FCM	Fuzzy C-means
FDM	Finite difference method
GA	Genetic algorithm
LSSVM	Least squares support vector machine
MDEA	Methyldiethanolamine
MEA	Monoethanolamine
ML	Machine learning
MLP	Multilayer perception
MNN	Maximum number of neurons
MOFs	Metal-organic frameworks
MSE	Mean squared error
Mw_a	Apparent Molecular weight
N_2	Nitrogen
P	Pressure
PSO	Particle swarm optimization
R^2	Coefficient of determination
RBF	Radial basis function
RMSE	Root mean squared error
STD	Standard deviation
T	Temperature
TEA	Triethanolamine
VLE	Vapor-liquid equilibrium

Symbols

x	Total concentration
α	Solubility capacity
g/mol	Gram/Mole
K	Degree of Kelvin
kPa	Kilo Pascal
wt%	Weight percentage
x1, 2	Input feature values
A1, 2	Fuzzy set of input variables x1
B1, 2	Fuzzy set of input variables x2
Oi	Output number (ANFIS)
μi	Membership function (ANFIS)
wi	Weight function (ANFIS)
$\overline{w}_i$	Normalized weight function (ANFIS)
fi	Function of the Sugeno-type fuzzy (ANFIS)
Π	Node (ANFIS)
xn	Input vectors (LSSVM)
yn	Output vectors (LSSVM)
b	Transposed form of the weight matrix (LSSVM)
w	Transposed form of the weight matrix (LSSVM)
f(x)	Decision function (LSSVM)
g(x)	Mapping data function (LSSVM)
ξ	Slack parameter (LSSVM)
α	Lagrange multipliers (LSSVM)
β	Lagrange multipliers (LSSVM)
$\mathbf{X_i^p}$	Input parameters (RBF)
$\mathbf{t^p}$	Target value (RBF)
N	Number of main functions (RBF)
∅	Activation function (RBF)
$\mathbf{f}(\mathbf{x})$	Radial basis function (RBF)
r	Distance between the x and data centers (RBF)
σ	Spread coefficient (RBF)

(Hussin and Aroua, 2019). As of today, no serious invention focusing on CO_2 capture using the adsorption methods has been reported, or the information is limited. To achieve techno-economic systems for this process, providing efficient adsorbents is important. There are satisfactory results from the experiments performed in the laboratory; however, applying the same methods to industrial scales remains a challenge (Hussin and Aroua, 2019).

For the process of CO_2 capture, various technologies can be used, as mentioned earlier (Amirkhani et al., 2020a). However, the most popular system is absorption by an amine-based solvent (Zhang et al., 2023a) mainly because it is inexpensive and can be used for relatively high flow rates of flue and industrial gases (Ghanbari-Kalajahi and Haghtalab, 2023). It should be noted that one of the differences between absorption and adsorption processes is that the former uses the total amount of the material used, but the latter uses the surface to occur. As mentioned earlier, the use of amine-based aqueous solutions in the process of absorption has grown and has been used significantly (He et al., 2023). In terms of cost and feasibility, there are limitations to the use of this process for post-combustion technologies. To begin with, the power which is used to compress the gas should be increased due to the low partial pressure of CO_2 in the flue gas outlet flow. The absorption column may not be large enough to support the large amounts of flue gases from plants (Dash and Wadibhasme, 2017). There are solutions to these issues, such as a quicker reaction between CO_2 and the solvent, a lower rate of degradation, and a larger solvent capacity (Sreedhar et al., 2017). For these reasons, blending amine solvents can be used to enhance the efficiency of the CO_2 capture process (Chen et al., 2022). By this method, we can boost the solubility at equilibrium and decrease the amount of energy used in the solvent regeneration process. The solubility of CO_2 in such systems has been studied previously by different research groups (Aghel et al., 2022).

The experimental methods to study absorption can be time-consuming and costly. Therefore, developing models to predict/estimate the absorption in this process is significantly helpful and can address different issues in process design (Zhong et al., 2023). That being said, modeling using AI, which is considered as one of the most practical methods of machine learning, has been very popular due to its valid, rapid and low-cost procedures, as well as being convenient to use (Dashti et al., 2021a).

Sipocz et al. suggested a feed-forward type of an ANN, which contains multilayers and analyzes the nonlinearity of input and output parameters (Sipöcz et al., 2011). In their study, they simulated the post-combustion CO_2 capture, which was based on amine. Another group presented the carbon dioxide content in aqueous blends containing piperazine, monoethanolamine, and triiso-propanolamine in partial pressure values below atmospheric pressure, and broad temperature and concentration ranges. Same group has used an ANN which estimates properties such as viscosity and corrosion. The efficiency of some neural networks, including radial basis function and back propagation multi-layer perceptron has been evaluated by Shahsavand et al. (2011). The experimental data of CO_2 capture by methyldiethanolamine and diethanolamine at several concentration values were used as the data required for training the algorithm. Another study estimated the thermal conductivity of ionic liquids based on properties such as the molecular weight of the liquid, pressure and temperature (Hezave et al., 2012). ANN has also been used in prediction of the level of sulfur in

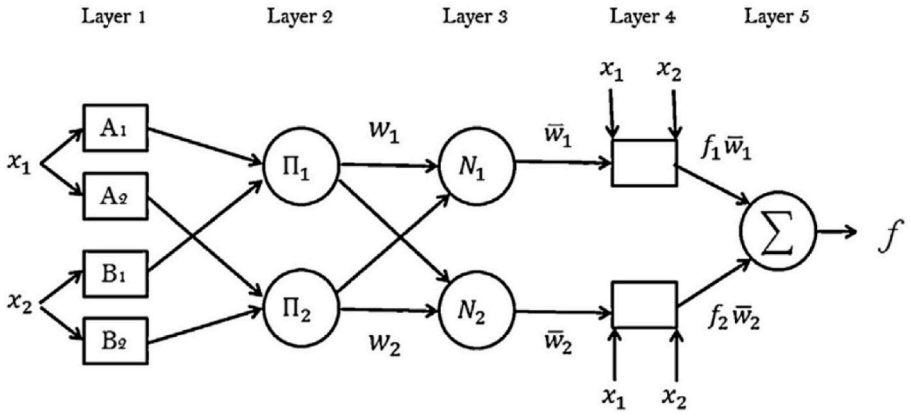

Fig. 1. Schematic of ANFIS architecture for a two-input x_1, y_1 and one output f. Copyright 2016, Reproduced with permission from (Ghiasi et al., 2016), Elsevier Science Ltd.

hydrogen sulfide at relatively high pressure and temperature values (Mohammadi and Richon, 2008).

Correlation equations based on empirical data were created to model the vapor-liquid equilibrium (VLE) and absorption rate of CO_2 in a ternary aqueous amine solvent. The model was incorporated into the PRO/II® commercial software using a user-added subroutine (Lee et al., 2019). Another study utilized 2D mathematical modeling with the finite difference method (FDM) to explore the impact of different ionic liquids, their concentrations, and liquid and gas flow rates on the CO_2 absorption process in membrane contactors (Darabi and Pahlavanzadeh, 2020). Gas mixture adsorption investigations involving metal-organic frameworks (MOFs) were conducted through molecular simulations. In this research, artificial neural networks (ANNs) were employed to predict the separation factor of CO_2 and CH_4, gas adsorption performance, and heat of adsorption (Yulia et al., 2021). To predict CO_2 solubility data in three types of aqueous amine blends, a new simplified Kent-Eisenberg model was developed. Additionally, a multilayer neural network model with the Levenberg-Marquardt backpropagation algorithm was created based on 500 reliable published experimental data (Li et al., 2022). In another approach, Nassef proposed a cost-efficient method that leverages AI and modern optimization techniques to enhance CO_2 solubility in carbon capture and storage (CCS) (Nassef, 2023).

Machine learning can be used as a robust approach to estimate different measures for the process of CO_2 equilibrium absorption (Liu et al., 2017). In this work, precise machine learning (ML)/AI models and algorithms have been developed to estimate the solubility of CO_2 in aqueous amines mixtures, including Hybrid-ANFIS, PSO-ANFIS, LSSVM, and GA-RBF which are known as high-speed and precise methods. The solubility estimations are based on the total concentration of the solution, apparent molecular weight, temperature and pressure, which are obtained using a relatively large set of experimental data. The accuracy of the developed models is so high.

2. Methodology

This section explains a theoretical description of the developed machine-learning models to estimate CO_2 sorption in blended amine solutions. The machine learning models are Hybrid-ANFIS, PSO-ANFIS, LSSVM, and GA-RBF.

2.1. ANFIS model

The adaptive neuro-fuzzy inference system (ANFIS) technique is usually used in highly nonlinear and complex systems because it involves both fuzzy inference systems and ANN methods (Amirkhani et al., 2022). This study implemented the Takagi-Sugeno fuzzy system using five layers and two inputs. The inputs and the single output of this algorithm are shown as x_1, x_2 and f. The equations below explain the common fuzzy rules (Dashti et al., 2020).

Rule 1:

$$\text{If } x_1 \text{ is } A_1 \text{ and } x_2 \text{ is } B_1 \text{ and etc.; then } f_1 = a_1x_1 + b_1x_2 + \ldots + r_1; \quad (1)$$

Rule 2:

$$\text{If } x_1 \text{ is } A_2 \text{ and } x_2 \text{ is } B_2 \text{ and etc.; then } f_2 = a_2x_1 + b_2x_2 + r_2; \quad (2)$$

where the consequent parameters are a_1, b_1, r_1, a_2, b_2, r_2. The parameters A_1, A_2, B_1, and B_2 represent the linguistic labels. This approach is based on a feed-forward neural network with five layers and different functions, which are shown in Equations (3)–(7). By having the inputs node in the first layer, the membership relation between inputs and outputs can be explained as:

$$O_{1,i} = \mu_{Ai}(x), i = 1, 2 \quad (3)$$

where, $O_{1,i}$ denotes the output of the ith node and μ_{Ai} represents a membership function (MF) like Gaussian MF.

In layer 2, every node is a constant node denoted as Π and the output of nodes within this layer is determined by computing the product of all incoming signals, as illustrated. is as shown below:

$$O_{2,i} = w_i = \mu_{Ai}(x) \times \mu_{Bi}(x), i = 1, 2 \quad (4)$$

In layer 3, the weight function would be normalized as shown below:

$$O_{3,i} = \overline{w}_i = \frac{w_i}{w_1 + w_2}, i = 1, 2 \quad (5)$$

Layer 4, also known as defuzzy layer, gives the product of the previous layer's output and the function of the Sugeno-type fuzzy rule:

$$O_{4,i=} \overline{w}_i f_i = \overline{w}_i (a_i x + b_i x_2 + \ldots + r_i), i = 1, 2 \quad (6)$$

In layer 5, we add all the outputs of the rules, as shown in Equation (7).

$$O_{5,i=} \sum_{i=1}^{n} \overline{w}_i f_i = \frac{\sum_i w_i f_i}{\sum_i w_i}, i = 1, 2 \quad (7)$$

More details about this method can be found elsewhere (Amirkhani et al., 2021). Fig. 1 Shows the schematic of ANFIS model.

2.2. CSA-LSSVM algorithm

Support Vector Machine (Vladimir and Vapnik, 1995) is a strong method which predicts nonlinear functions and can also be used in classification problems (Dashti et al., 2021b), including difficult and

Table 1
Details of the PSO-ANFIS model for estimating the CO_2 solubility.

Parameter	Value
Iterations	500
No. of particles	1000
W_{min}	0.5
W_{damp}	0.99
C_1	1
C_2	2
Number of fuzzy rules	10

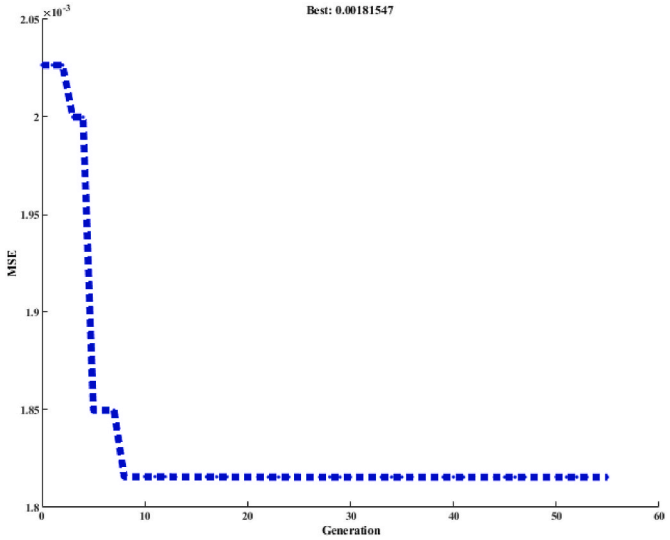

Fig. 2. The convergent of GA to the optimum model.

complex ones. This technique deals with mapping a set of experimental data points which are nonlinearly mapped into a higher dimensional space. This data set can be shown as $\{(x_1, y_1), \ldots, (x_n, y_n)\}$, where x_i and y_i represent input and output vectors, respectively. In this study, the output parameter is solubility. The main goal of the support vector machine method is to find the best hyper-plane in classification, which maintains the minimum distance from the data points (Suykens and Vandewalle, 1999). In this method, the decision function in the case of linearity in data classification can be written as (Chamkalani et al., 2014):

$$f(x) = w^t g(x) + b \tag{8}$$

where b and w represent the transposed form of the weight matrix, and g (x) indicates the function used for mapping the data. Provided that the difference in data from the two categories is recognizable, the conditions the value of the above function is subjected are as follows:

$$\begin{cases} f(x_i) \geq 1 & if\ y_i = +1 \\ f(x_i) \geq -1 & if\ y_i = -1 \end{cases} \tag{9}$$

Some of the data used for training the algorithm form the support vectors provided that the conditions above are satisfied (Cristianini and Shawe-Taylor, 2000). If the case of interest deals with problems with linear separation capacity in the feature margin, there would be a limitless number of decision functions, all meeting the conditions above. A proper dividing plane is the hyper-plane, which has the maximum distance from the plane that passes the data points. An ideal separator is a plane that gives the highest margin and lowest noise utilising slack margin as follows (Cristianini and Shawe-Taylor, 2000):

$$\min\left(\frac{1}{2}\|w\|^2\right) + C\sum_{i=1}^{n}\xi_i \tag{10}$$

In Equation (10), ξ and C represent the slack parameter and a constant. The former shows the difference between the data in their corresponding inaccurate and actual categories. The latter parameter, which has a positive value, shows a compromise between the highest margin and the minimum error. This deterministic strategy deals with convex optimization, for which the method of Lagrange multipliers was used to solve it (Baylar et al., 2009):

$$g(w,b,\alpha,\xi,\beta) = \frac{1}{2}\ w^t w + \frac{C}{2}\sum_{i=1}^{n}\xi_i - \sum_{i=1}^{n}\alpha_i(y_i[w^t x_i + b] - 1 + \xi_i)\Big) - \sum_{i=1}^{n}\beta_i\xi_i \tag{11}$$

where α and β parameters are the Lagrange multipliers, we can deal with this problem using the Lagrangian Saddle Point when the values assigned to α_i are positive. In order to address the linearity and nonlinearity of the cases, and also because of the specific form of the support vector machine algorithm, the practical approach is to obtain sparse solutions (Suykens and Vandewalle, 1999).

In order to do a convex optimization, support vectors are created, and to do tasks such as predicting the functions or performing regressions. We can use the support vector machine method. To do so, we use quadratic programming subject to inequality constraints. Due to the constraints in the optimization part of the model, estimating the functions through the support vector machine approach is considered computationally expensive (Wang and Hu, 2005). This method is time-consuming for an extensive set of functions (Wang and Hu, 2005).

2.3. Radial basis function neural network (RBF-NN)

The radial basis function network is among one of the most popular ANN algorithms due to its high precision and sufficiently good performance. In these algorithms, radial basis functions are, in fact, activation functions. The application of these networks is expanded to various areas, for example, system control, clustering, pattern classification, time series forecasting, spline interpolation and function approximation. In most cases, there are three layers in RBF-NNs: input, single hidden, and output layers (Tatar et al., 2016). Unlike the modeling procedure of RBF and MLP neural networks, there are similarities in the structure of these two algorithms (Tatar et al., 2013).

In RBF-NN, the weights are obtained in the training phase. Selecting and optimizing the parameters involved in the algorithm is considered a significant task that can lead to a sufficiently precise estimation (Park and Sandberg, 1991).

A lot of difficult mapping problems can be answered by RBF-NNs using intermediate layers. Typically, upon any variation in data, the statistical approaches correct the variables in the network accordingly. RBF-NNs share some features, including (Chen et al., 1991).

(i) In the training phase, the weights are assigned from the input to the hidden layer and, after that, from the hidden to the output layer.
(ii) The networks are able to ideally interpolate the data.
(iii) The output nodes utilize linear summation functions.
(iv) Some sorts of radial basis functions, for example, Gaussian, are applied by hidden nodes.
(v) The training phase takes less time to be completed than in standard ANN approaches.

The function f(x) can be defined as $f(X^p) = t^p \forall p = 1, \ldots, D$, where $X^p = [X_i^p : 1, 2, \ldots, N]$), which has D dimensions, indicates the input parameters. Also, N shows the number of data points and t^p represents the target value, on which X^p is projected using RBF. There are N main

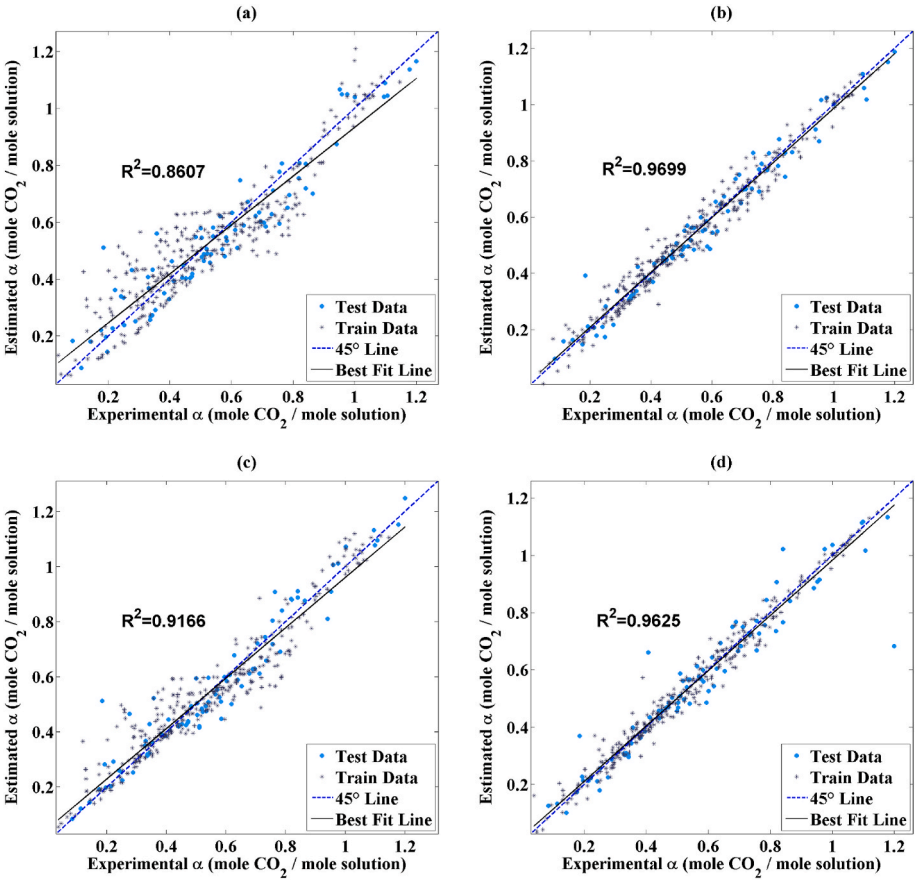

Fig. 3. Regression plot for the solubility of CO_2 prognostication by (a) ANFIS, (b) PSO-ANFIS, (c) LSSVM and (d) GA-RBF.

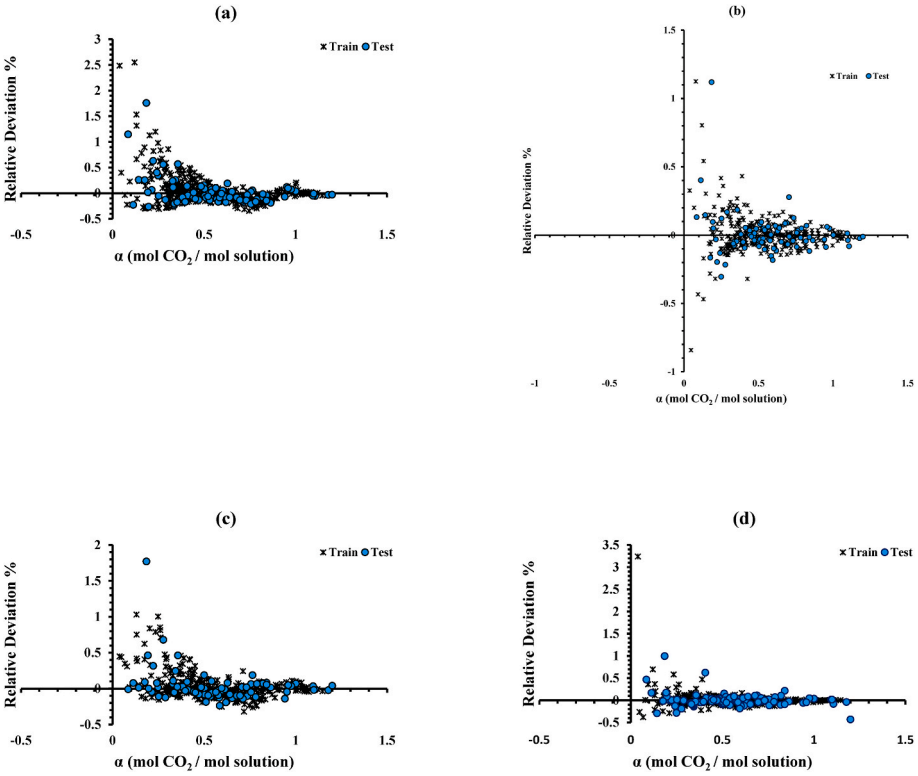

Fig. 4. Relative deviation of the estimated CO_2 solubility values for both test and train data points by (a) Hybrid-ANFIS, (b) PSO-ANFIS, (c) LSSVM and (d) GA-RBF.

Table 2
Estimation accuracy of different models.

Model			
Parameters	Train	Test	Total
Hybrid-ANFIS			
R^2	0.8481	0.9031	0.8607
MSE	0.0089	0.0067	0.0085
STD	0.2232	0.2475	0.2284
%AARD	19.18	16.45	18.63
PSO-ANFIS			
R^2	0.9705	0.9678	0.9699
MSE	0.0017	0.0022	0.0018
STD	0.2391	0.2589	0.2434
%AARD	8.17	8.545	8.25
LSSVM			
R^2	0.9132	0.9288	0.9166
MSE	0.0051	0.0050	0.0051
STD	0.2284	0.2611	0.2356
%AARD	12.41	11.43	12.22
GA-RBF			
R^2	0.9794	0.9054	0.9625
MSE	0.0012	0.0065	0.0023
STD	0.2395	0.2535	0.2426
%AARD	7.00	9.70	7.54

functions of this type involved in RBF-NN, presented as $\varnothing\ (\|x - x^p\|)$ in hidden layer nodes. The activation function is indicated by $\varnothing$, which is nonlinear and dependent on the difference between x and x^p. $\|x - x^p\|$ is the Euclidean norm and represents this difference. The basis function is $f(x) = \sum_{p=1}^{N} w_p \varnothing(\|x - x^p\|)$ and is obtained by linearly combining a number of basic functions (Halali et al., 2016).

Based on both observation and theory, not all the features of the interpolation function depend on the type of $\varnothing(r)$. Here was used the Gaussian form of this function, which is well-known and acceptable for this study and is defined as (Halali et al., 2016):

$$\varnothing(r) = \exp\left(-\frac{\sigma^2}{r^2}\right) \tag{12}$$

where r shows how far the point x and center are from each other, and σ, which is a positive value, represents the width and shows how flat the function is. RBF-NNs have been widely studied by other groups as well (Barati-Harooni et al., 2016).

3. Data collection and analysis

In this study, the data on the solubility of CO_2 were gathered from the experiments done by other groups. The solubility data were obtained under different conditions. The 413 data points were separated into training and test sets. Due to several reasons such as unreliable data or unconsidered parameters in tests such as humidity and purity or grades of amines, these data could not correlate well by ML models. The former set contains around 80% of the available experimental data, while the rest forms the test set. The solutions corresponding to each set are the same. The operating conditions are dissimilar. The test set assesses the performance of the algorithm based on any given inputs.

One significant step is determining the independent parameters related to the correlation, which occurs before the training phase. The model should be able to differentiate between various types of aqueous solutions in blends. As mentioned earlier, the conditions at which the data are acquired should be considered. The solubility of CO_2 depends on parameters, such as the set of temperature (K), the total concentration (wt. %), pressure of CO_2 (kPa) and its apparent molecular weight (g/mol). Note that the type of the solution and its concentration affect the apparent molecular weight, which is often used to reduce the computational effort. In the developed algorithm, the input parameters are apparent molecular weight, the pressure of CO_2, total concentration and temperature:

$$\alpha = f(T, x, P_{CO_2}, \mathrm{Mw_a}) \tag{13}$$

The apparent molecular weight is defined as:

$$\mathrm{MW_a} = \sum_{i=1}^{\mathrm{NC}} x_i \mathrm{MW}_i \tag{14}$$

where i and NC represent the counter and the number of components.

4. Results and discussion

In this section, details and necessary explanations about the methods for the development of models are described. In addition, different models performances are compared by statistical and graphical methods, and their applicability in the estimation of real data is assessed.

4.1. Model development

The MLP-ANN algorithm includes four neurons in the input and one in the output layer. That being said, in the developed algorithm, the count of neurons in the hidden layer was altered from one to thirty. It was observed that the multilayer perceptron algorithm gives the best accuracy with a hidden layer containing 28 neurons, which corresponds to the best efficiency.

According to other research work, estimating the membership functions is not a straightforward task to be done using any specific equation. As a result, to do so, the trial and error method is suggested. The Gaussian membership function, which other researchers have also used, gave the best results. It should be noted that seventeen rules were incorporated in the ANFIS based on the Fuzzy C-means method. The ANFIS membership functions associated with the input parameters can be seen in Fig. S1 (supplementary information). For the training phase, the number of epochs was selected as 2000. Also, in the beginning, hybrid learning was used to estimate the parameters.

The PSO-ANFIS model is based on finding the optimum parameters of ANFIS, which can be obtained using the PSO algorithm (Kennedy and Eberhart, 1995). MATLAB software was used to set up the PSO-ANFIS algorithm. This algorithm uses PSO to help the hybrid model better correlate the inputs and output. This model can have high accuracy, especially in the case of non-linearity, and therefore can improve the algorithm's efficiency. As mentioned earlier, the particle swarm optimization parameters should be properly selected. The trial and error method was applied (Table 1). Fig. S2 (supplementary information) demonstrates the PSO-ANFIS membership functions associated with the input parameters.

The tuning or penalty parameters used in the LSSVM approach are σ^2 and γ. A frequently used optimization approach is CSA (Xavier-de-Souza et al., 2009), which gives a satisfactory data fit. Applying the coupled CSA algorithm in this study gave us the optimised values of σ^2 and γ as 10.17 and 4761454.1, respectively.

In RBF, the Maximum Number of Neurons (MNN) and Spread are known as the key hyperparameters, which directly affect the precision and efficiency of the algorithm. There are multiple methods to obtain the optimised values of these parameters, such as trial and error. The trial and error method is normally challenging and takes a lot of time to give the desired results, especially for a nonlinear algorithm such as RBF. GA (Hassan et al., 2005) was used as a strong and robust tool for obtaining the optimised values of the above-mentioned hyperparameters. The best values of MNN and Spread, which were calculated after 55 generations, are 91 and 99.514, respectively. Fig. 2 presents how the GA algorithm converges to the mentioned optimum values by showing MSE variations versus generation sequences. It is clear that these values were obtained after 55 generations.

Table 3
Details of the data used in this study, and the AARD% of the developed models for each blended amine solution.

No.	Mixed aqueous solution type (wt. %)	Pressure range (kPa)	Temp. range (K)	Apparent molecular weight (g/mol)	Overall concentration range (wt. %)	No. data	%AARD				Ref.
							ANFIS	PSO-ANFIS	LSSVM	GARBF	
1	(24.0 %) MEA + (6.0 %) TEA	1.07–122	313.2–373.2	36.22–52.08	30–30	140	14.40	6.30	9.46	3.94	Cheng et al. (2010)
2	(18.0 %) MEA + (12.0 %) TEA						13.73	6.77	7.24	6.85	
3	(12.0 %) MEA + (18.0 %) TEA						17.86	6.91	10.16	5.98	
4	(6.0 %) MEA + (24.0 %) TEA						24.71	11.19	13.56	7.84	
5	(1.5 %) DEA + (28.5 %) AMP	1.92–92.77	303–323	39.59–40.31	30–30	59	13.54	8.43	7.20	8.42	(Kundu and Bandyopadhyay, 2006)
6	(3.0 %) DEA + (27.0 %) AMP						15.15	5.88	10.40	6.42	
7	(4.5 %) DEA + (25.5 %) AMP						16.87	5.44	10.82	5.34	
8	(6.0 %) DEA + (24.0 %) AMP						15.09	5.62	10.18	5.82	
9	(6.0 %) DEA + (24.0 %) AMP	1.61–364.9	313.15–353.15	40.31–42.23	30–30	46	24.25	11.74	19.60	9.07	(Seo and Hong, 1996)
10	(12.0 %) DEA + (18.0 %) AMP						8.42	4.11	8.72	4.14	
11	(18.0 %) DEA + (12.0 %) AMP						10.72	4.45	9.16	5.05	
12	(25.0 %) DEA + (5.0 %) AMP	2.8–2908	313.15–393.15	41.90–62.13	25–45	69	7.67	4.19	5.66	5.78	(Murrieta-Guevara et al., 1998b)
13	(20.0 %) DEA + (10.0 %) AMP						13.37	9.44	10.21	7.84	
14	(10.0 %) DEA + (15.0 %) MDEA						23.50	8.83	17.86	9.60	
15	(10.0 %) DEA + (20.0 %) MDEA						15.79	5.36	14.97	3.36	
16	(20.0 %) DEA + (10.0 %) MDEA						31.34	19.68	32.21	17.49	
17	(10.0 %) DEA + (35.0 %) MDEA						43.14	11.57	35.67	11.24	
18	(10.0 %) DEA + (20.0 %) MDEA						79.13	11.35	11.69	58.90	
19	(12.5 %) DEA + (32.5 %) MDEA	0.4–1999.1	313.15–393.15	61.78–68.89	45–55	99	21.67	14.00	15.40	7.70	(Rebolledo-Libreros, M. a.E. and Trejo, A.J.F.p. e., 2004)
20	(12.5 %) DEA + (32.5 %) MDEA + (4.0 %) AMP						20.26	8.32	14.26	9.26	
21	(12.5 %) DEA + (32.5 %) MDEA + (6.0 %) AMP						13.55	6.45	11.11	3.90	
22	(12.5 %) DEA + (32.5 %) MDEA + (10.0 %) AMP						14.40	10.59	10.56	3.53	
	Total	**0.4–2908**	**303–393.15**	**36.22–68.89**	**25–55**	**413**	**18.63**	**8.25**	**12.22**	**7.54**	

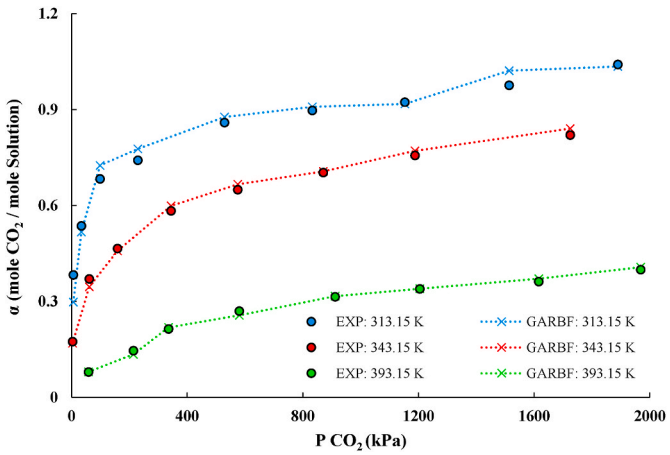

Fig. 5. Solubility of CO_2 in an aqueous solution of 32.5 wt% MDEA, 12.5 wt% DEA and 10 wt% AMP at different temperatures and its estimation using GA-RBF.

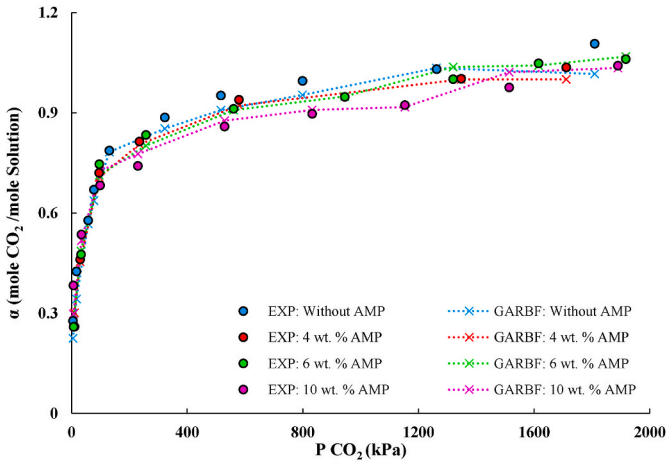

Fig. 6. Solubility of CO_2 at 313.15 K, in an aqueous solution of 32.5 wt% MDEA and 12.5 wt% DEA: without AMP; with 4 wt% AMP; with 6 wt% AMP and with 10 wt% AMP and its estimation using GA-RBF.

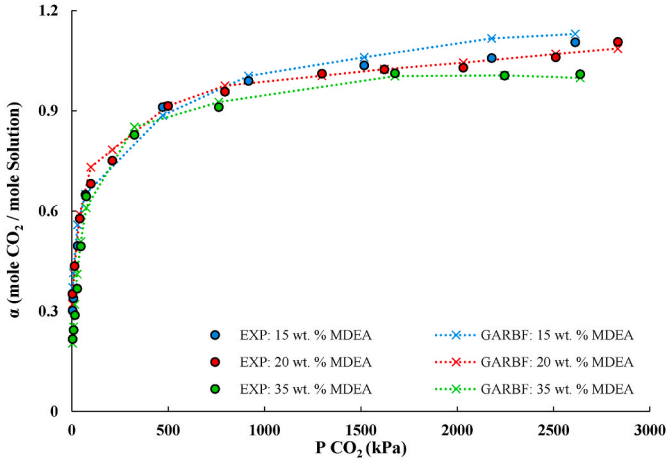

Fig. 7. Solubility of CO_2 at 313.15 K, in an aqueous solution of 10 wt% DEA: with 15 wt% MDEA; with 20 wt% MDEA and with 35 wt% MDEA and its estimation using GA-RBF.

4.2. Finding the best approach

In this section, the efficiency and capability of different models were compared. To evaluate the accuracy of the proposed models, four statistical parameters were used: correlation factor (R^2), standard deviation (STD), root mean squared error (RMSE), and average absolute relative deviation (AARD). The formulas for these parameters are given below.

$$R^2 = 1 - \frac{\sum_{i=1}^{n}\left[x_i^{estimated} - x_i^{experimental}\right]^2}{\sum_{i=1}^{n}\left[x_i^{estimated} - x^m\right]^2}, x_m = \frac{\sum_{i=1}^{n} x_i^{experimental}}{n} \quad (15)$$

$$AARD\% = \frac{100}{n}\sum_{i=1}^{n}\frac{\left|x_i^{estimated} - x_i^{experimental}\right|}{x_i^{experimental}} \quad (16)$$

$$MSE = \frac{1}{n}\sum_{i=1}^{n}\left(x_i^{experimental} - x_i^{estimated}\right)^2 \quad (17)$$

$$STD = \sqrt{\sum_{i=1}^{n}\left(\frac{\left(x_i^{estimated} - x_m\right)^2}{n}\right)} \quad (18)$$

Fig. 3 shows the regression values, which also verify the validity of the four approaches. This means that the models were not over- or undertrained. Hybrid-ANFIS, PSO-ANFIS, LSSVM, and GA-RBF techniques have the R^2 values of 0.8607, 0.9699, 0.9166 and 0.9625, respectively.

Fig. S3(supplementary information) shows the trend plots for three phases of trained and tested data points of the developed model. This figure clarifies the precision and the enhancement of the improved model. It also exhibits the anticipations of the executed model track the trend of reported data with a satisfactory accuracy. Fig. 4 shows the relative deviations between the estimated values from each approach and actual data. We can see that the deviation values are mostly close to zero, confirming a good agreement between the estimated results and experimental data. In addition, it is concluded that GA-RBF approach has a higher efficiency than the rest of the methods.

The values of the MSE, standard deviation, AARD% and R^2 were calculated to compare the efficiency and accuracy of the mentioned methods, as shown in Table 2. Lower values of AARD% (near zero) and higher values of R^2 (near 1), shows the best and accurate model. As a result, GA-RBF and PSO-ANFIS models with R^2 value of 0.9054 and 0.9678 and AARD% of 9.70 and 8.55 (for test data) show the best accuracy as well as the fastest convergence in estimating the solubility of CO_2.

Table 3 shows the details of employed data, and the AI models AARD % values for estimating the CO_2 absorption in blended amine solution. Table 3 demonstrates that GA-RBF accuracy is higher than other models in the case of solutions no. 1, 3, 4, 5, 7, 9, 13, 15, 16, 17, 19, 21 and 22. Table 3 clearly indicates that in the case of blended amine solutions no. 2, 6, 8, 10, 11, 12, 14, 18 and 20, the AARD% of the PSO-ANFIS model is lower than the GA-RBF model. LSSVM accuracy in the case of blended amine solution no.5 is higher than in other models.

Figs. 5–7 indicate a trend of the general behaviour of the developed models and experimental results. It can be seen that estimated and experimental data are in good agreement. It can be inferred that (a) at constant temperature and composition, and the CO_2 absorption raises with elevating pressure (b) at constant pressure and composition, the CO_2 absorption reduces with rising temperature and (c) at constant temperature and concentration in the ternary mixture, the increase in concentration significantly increases the CO_2 loading capacity of the aqueous blended amine system. Fig. 6 indicates the impacts of adding AMP in various concentrations to the aqueous solution of 32.5 wt% MDEA and 12.5 wt% DEA in the solubility data for CO_2 at 313.15 K. As can be seen, CO_2 absorption rises by the increment of the concentration of AMP. This obviously demonstrates the pros of having the third alkanolamine in the solution of MDEA with DEA (Rebolledo-Libreros

and Trejo, 2004). Fig. 7. Shows the effect of adding MDEA to DEA + MDEA solution. It is evident that MDEA has a limited impact on CO_2 absorption, especially at elevated pressures. It is well-established that the reactivity towards CO_2 follows the order of primary (AMP) > secondary (DEA) > tertiary (MDEA) alkanolamines. It demonstrates that blending amine with AMP are more effective to those with MDEA (Murrieta-Guevara et al., 1998b).

The optimal amine mixture can be determined using the data collected in this study. As depicted in Table S1 of the supplementary data, it is evident that a solution comprising 25% DEA and 5% AMP yields the highest CO_2 absorption, reaching 1.2 mole of CO_2 per mole of alkanolamine. This maximum loading was achieved under the conditions of a pressure of 2908 kPa and a temperature of 298 K. (Murrieta-Guevara et al., 1998a).

5. Conclusions

In this work, several machine learning approaches, namely Hybrid-ANFIS, PSO-ANFIS, LSSVM and GA-RBF, were used to estimate the solubility of CO_2 in binary and ternary amines aqueous solutions. The blinded amine solutions were blends of ethanolamine (MEA), triethanolamine (TEA), aminomethyl propanol (AMP), methyl diethanolamine (MDEA). The solubility was changed by different factors, including partial pressure of CO_2 (kPa), apparent molecular weight (g/mol), total concentration (wt. %), and temperature (K) of the solutions. These parameters were the inputs to the algorithm, which can be used over large ranges of pressure and temperature values corresponding to various blends. The performances of the AI methods were assessed, and the GA-RBF method results in an AARD% of 7.54. The utilization of GA-RBF with exceptional accuracy demonstrates the novelty and reliability of this model. A key benefit of this algorithm is its capability to handle intricate relationships between CO_2 concentration and solubility without being constrained by factors like concentration and temperature. The findings from this research can serve as a valuable resource for scientists seeking to determine CO_2 solubility in aqueous solutions containing commonly used blended amines. This eliminates the need for expensive experimental work, and researchers can confidently rely on this data due to its validation through prior experimental studies. Moreover, these models can assist researchers in the design and management of CO_2 capture plant systems. The latter factor is particularly of great significance when dealing with big data. Another advantage of this approach is the ability to handle a relatively large amount of input data.

CRediT authorship contribution statement

Farid Amirkhani: Conceptualization, Methodology, Software, Writing – original draft, Resources. **Amir Dashti:** Conceptualization, Methodology, Software, Writing – original draft, Resources. **Mojtaba Jokar:** Data curation, Formal analysis, Writing – original draft. **Amir H. Mohammadi:** Writing – review & editing. **Abdoulmohammad Gholamzadeh Chofreh:** Conceptualization, Writing – review & editing. **Petar Sabev Varbanov:** Supervision, Project administration, Conceptualization. **John L. Zhou:** Conceptualization, Writing – review & editing.

Declaration of competing interest

The authors declare that they have no known competing financial interests or personal relationships that could have appeared to influence the work reported in this paper.

Data availability

Data will be made available on request.

Appendix A. Supplementary data

Supplementary data to this article can be found online at https://doi.org/10.1016/j.jclepro.2023.139435.

References

Aghel, B., Janati, S., Wongwises, S., Shadloo, M.S., 2022. Review on CO2 capture by blended amine solutions. Int. J. Greenh. Gas Control 119, 103715.

Amirkhani, F., Dashti, A., Abedsoltan, H., Mohammadi, A.H., Chau, K.-W., 2021. Towards estimating absorption of major air pollutant gasses in ionic liquids using soft computing methods. J. Taiwan Inst. Chem. Eng. 127, 109–118.

Amirkhani, F., Dashti, A., Abedsoltan, H., Mohammadi, A.H., Chofreh, A.G., Goni, F.A., Klemeš, J.J., 2022. Estimating flashpoints of fuels and chemical compounds using hybrid machine-learning techniques. Fuel 323, 124292.

Amirkhani, F., Harami, H.R., Asghari, M., 2020a. CO2/CH4 mixed gas separation using poly (ether-b-amide)-ZnO nanocomposite membranes: experimental and molecular dynamics study. Polym. Test. 86, 106464.

Amirkhani, F., Mosadegh, M., Asghari, M., Parnian, M.J., 2020b. The beneficial impacts of functional groups of CNT on structure and gas separation properties of PEBA mixed matrix membranes. Polym. Test. 82, 106285.

Barati-Harooni, A., Najafi-Marghmaleki, A., Tatar, A., Mohammadi, A.H., 2016. Experimental and modeling studies on adsorption of a nonionic surfactant on sandstone minerals in enhanced oil recovery process with surfactant flooding. J. Mol. Liq. 220, 1022–1032.

Baylar, A., Hanbay, D., Batan, M., 2009. Application of least square support vector machines in the prediction of aeration performance of plunging overfall jets from weirs. Expert Syst. Appl. 36 (4), 8368–8374.

Ben-Mansour, R., Habib, M., Bamidele, O., Basha, M., Qasem, N., Peedikakkal, A., Laoui, T., Ali, M., 2016. Carbon capture by physical adsorption: materials, experimental investigations and numerical modeling and simulations–a review. Appl. Energy 161, 225–255.

Chamkalani, A., Zendehboudi, S., Bahadori, A., Kharrat, R., Chamkalani, R., James, L., Chatzis, I., 2014. Integration of LSSVM technique with PSO to determine asphaltene deposition. J. Petrol. Sci. Eng. 124, 243–253.

Chen, G., Chen, G., Peruzzini, M., Zhang, R., Barzagli, F., 2022. Understanding the potential benefits of blended ternary amine systems for CO2 capture processes through 13C NMR speciation study and energy cost analysis. Separ. Purif. Technol. 291, 120939.

Chen, S., Cowan, C., Grant, P., 1991. Orthogonal least squares learning algorithm for radial. IEEE Trans. Neural Network. 2 (2), 303.

Cheng, M.-D., Caparanga, A.R., Soriano, A.N., Li, M.-H., 2010. Solubility of CO2 in the solvent system (water+ monoethanolamine+ triethanolamine). J. Chem. Therm. 42 (3), 342–347.

Cristianini, N., Shawe-Taylor, J., 2000. An Introduction to Support Vector Machines and Other Kernel-Based Learning Methods. Cambridge University Press.

Darabi, M., Pahlavanzadeh, H., 2020. Mathematical modeling of CO2 membrane absorption system using ionic liquid solutions. Chemical Engineering and Processing-Process Intensification 147, 107743.

Dash, S.K., Wadibhasme, L.H., 2017. Retrofitting a CO2 capture unit with a coal based power plant, process simulation and parametric study. Journal of Clean Energy Technologies 5 (3).

Dashti, A., Amirkhani, F., Hamedi, A.-S., Mohammadi, A.H., 2021a. Evaluation of CO2 absorption by amino acid salt aqueous solution using hybrid soft computing methods. ACS Omega 6 (19), 12459–12469.

Dashti, A., Bahrololoomi, A., Amirkhani, F., Mohammadi, A.H., 2020. Estimation of CO2 adsorption in high capacity metal− organic frameworks: applications to greenhouse gas control. J. CO2 Util. 41, 101256.

Dashti, A., Mazaheri, O., Amirkhani, F., Mohammadi, A.H., 2021b. Molecular descriptors-based models for estimating net heat of combustion of chemical compounds. Energy 217, 119292.

Ghanbari-Kalajahi, H., Haghtalab, A., 2023. Vapor-liquid equilibrium of carbon dioxide solubility in a deep eutectic solvent (choline chloride: MDEA) and a mixture of DES with piperazine-experimental study and modeling. J. Mol. Liq. 375, 121310.

Ghiasi, M.M., Arabloo, M., Mohammadi, A.H., Barghi, T., 2016. Application of ANFIS soft computing technique in modeling the CO2 capture with MEA, DEA, and TEA aqueous solutions. Int. J. Greenh. Gas Control 49, 47–54.

Halali, M.A., Azari, V., Arabloo, M., Mohammadi, A.H., Bahadori, A., 2016. Application of a radial basis function neural network to estimate pressure gradient in water–oil pipelines. J. Taiwan Inst. Chem. Eng. 58, 189–202.

Hassan, R., Cohanim, B., De Weck, O., Venter, G., 2005. A Comparison of Particle Swarm Optimization and the Genetic Algorithm. In: AIAA/ASME/ASCE/AHS/ASC Structures, Structural Dynamics and Materials Conference, 46th, 1897.

He, X., He, H., Barzagli, F., Amer, M.W., Li, C.e., Zhang, R., 2023. Analysis of the energy consumption in solvent regeneration processes using binary amine blends for CO2 capture. Energy 270, 126903.

Hezave, A.Z., Raeissi, S., Lashkarbolooki, M., 2012. Estimation of thermal conductivity of ionic liquids using a perceptron neural network. I&EC Res.51 (29),, 9886–9893.

Hussin, F., Aroua, M.K., 2019. Recent trends in the development of adsorption technologies for carbon dioxide capture: a brief literature and patent reviews (2014-2018). J. Clean. Prod., 119707

Kennedy, J., Eberhart, R., 1995. Particle Swarm Optimization (PSO), Proc. IEEE International Conference on Neural Networks, Perth, Australia, pp. 1942–1948.

Kundu, M., Bandyopadhyay, S.S., 2006. Solubility of CO2 in Water+ Diethanolamine+ 2-Amino-2-methyl-1-propanol. J. Chem. Eng. Data 51 (2), 398–405.
Lee, J., Kim, J., Kim, H., Lee, K.S., Won, W., 2019. A new modeling approach for a CO2 capture process based on a blended amine solvent. J. Nat. Gas Sci. Eng. 61, 206–214.
Li, H.J., 2023. CO2 capture by various nanoparticles: recent development and prospective. J. Clean. Prod., 137679
Li, T., Yang, C., Tantikhajorngosol, P., Sema, T., Shi, H., Tontiwachwuthikul, P., 2022. Experimental investigations and the modeling approach for CO2 solubility in aqueous blended amine systems of monoethanolamine, 2-amino-2-methyl-1-propanol, and 2-(butylamino) ethanol. Environ. Sci. Pollut. Control Ser. 29 (46), 69402–69423.
Li, T., Yu, Q., Barzagli, F., Li, C.e., Che, M., Zhang, Z., Zhang, R., 2023. Energy Efficient Catalytic CO2 Desorption: Mechanism, Technological Progress and Perspective. Carbon Capture Science & Technology, 100099.
Liu, Z., Li, H., Liu, K., Yu, H., Cheng, K., 2017. Design of high-performance water-in-glass evacuated tube solar water heaters by a high-throughput screening based on machine learning: a combined modeling and experimental study. Sol. Energy 142, 61–67.
Mohammadi, A.H., Richon, D., 2008. Estimating sulfur content of hydrogen sulfide at elevated temperatures and pressures using an artificial neural network algorithm. I&EC Res. 47 (21), 8499–8504.
Mosadegh, M., Amirkhani, F., Harami, H.R., Asghari, M., Parnian, M.J., 2020. Effect of Nafion and APTEOS functionalization on mixed gas separation of PEBA-FAU membranes: experimental study and MD and GCMC simulations. Separ. Purif. Technol. 247, 116981.
Murrieta-Guevara, F., Rebolledo-Libreros, M.E., Romero-Martinez, A., Trejo, A., 1998a. Solubility of CO2 in aqueous mixtures of diethanolamine with methyldiethanolamine and 2-amino-2-methyl-1-propanol. Fluid Phase Equil. 150, 721–729.
Murrieta-Guevara, F., Rebolledo-Libreros, M.E., Romero-Martinez, A., Trejo, A., 1998b. Solubility of CO2 in aqueous mixtures of diethanolamine with methyldiethanolamine and 2-amino-2-methyl-1-propanol. Fluid Phase Equil. 150, 721–729.
Nassef, A.M., 2023. Improving CO2 absorption using artificial intelligence and modern optimization for a sustainable environment. Sustainability 15 (12), 9512.
Olajire, A.A., 2018. Recent progress on the nanoparticles-assisted greenhouse carbon dioxide conversion processes. J. CO2 Util. 24, 522–547.
Park, J., Sandberg, I.W., 1991. Universal approximation using radial-basis-function networks. Neural Comput. 3 (2), 246–257.
Rebolledo-Libreros, M.a.E., Trejo, A., 2004. Gas solubility of CO2 in aqueous solutions of N-methyldiethanolamine and diethanolamine with 2-amino-2-methyl-1-propanol. Fluid Phase Equil. 218 (2), 261–267.
Safdarnejad, S.M., Hedengren, J.D., Baxter, L.L., 2015. Plant-level dynamic optimization of Cryogenic Carbon Capture with conventional and renewable power sources. Appl. Energy 149, 354–366.
Seo, D.-J., Hong, W.-H., 1996. Solubilities of carbon dioxide in aqueous mixtures of diethanolamine and 2-amino-2-methyl-1-propanol. J. Chem. Eng. Data 41 (2), 258–260.
Shahsavand, A., Fard, F.D., Sotoudeh, F., 2011. Application of artificial neural networks for simulation of experimental CO2 absorption data in a packed column. J. Nat. Gas Sci. Eng. 3 (3), 518–529.
Sipöcz, N., Tobiesen, F.A., Assadi, M., 2011. The use of artificial neural network models for CO2 capture plants, Applied Energy, 88 (7), 2368–2376.
Sreedhar, I., Nahar, T., Venugopal, A., Srinivas, B., 2017. Carbon capture by absorption–path covered and ahead. Renew. Sustain. Energy Rev. 76, 1080–1107.
Suykens, J.A., Vandewalle, J., 1999. Least squares support vector machine classifiers. Neural Process. Lett. 9 (3), 293–300.
Tatar, A., Barati, A., Yarahmadi, A., Najafi, A., Lee, M., Bahadori, A., 2016. Prediction of carbon dioxide solubility in aqueous mixture of methyldiethanolamine and N-methylpyrrolidone using intelligent models. Int. J. Greenh. Gas Control 47, 122–136.
Tatar, A., Shokrollahi, A., Mesbah, M., Rashid, S., Arabloo, M., Bahadori, A., 2013. Implementing radial basis function networks for modeling CO2-reservoir oil minimum miscibility pressure. J. Nat. Gas Sci. Eng. 15, 82–92.
Vladimir, V.N., Vapnik, V., 1995. The Nature of Statistical Learning Theory. Springer Heidelberg.
Wang, H., Hu, D., 2005. Comparison of SVM and LS-SVM for Regression, 2005 International Conference on Neural Networks and Brain. IEEE, pp. 279–283.
Xavier-de-Souza, S., Suykens, J.A., Vandewalle, J., Bollé, D., 2009. Coupled simulated annealing. IEEE Transactions on Systems, Man, and Cybernetics, Part B (Cybernetics) 40 (2), 320–335.
Yulia, F., Chairina, I., Zulys, A., 2021. Multi-objective genetic algorithm optimization with an artificial neural network for CO2/CH4 adsorption prediction in metal–organic framework. Therm. Sci. Eng. Prog. 25, 100967.
Zhang, R., Li, Y., He, X., Niu, Y., Li, C.e., Amer, M.W., Barzagli, F., 2023a. Investigation of the improvement of the CO2 capture performance of aqueous amine sorbents by switching from dual-amine to trio-amine systems. Separ. Purif. Technol. 316, 123810.
Zhang, R., Li, Y., Zhang, Y., Li, T., Yang, L., Li, C.e., Barzagli, F., Zhang, Z., 2023b. Energy-saving effect of low-cost and environmentally friendly sepiolite as an efficient catalyst carrier for CO2 capture. ACS Sustain. Chem. Eng. 11 (11), 4353–4363.
Zhang, R., Liu, R., Barzagli, F., Sanku, M.G., Li, C.e., Xiao, M., 2023c. CO2 absorption in blended amine solvent: speciation, equilibrium solubility and excessive property. Chem. Eng. J. 466, 143279.
Zhong, X., Li, C.e., Hu, X., Zhang, R., 2023. A modified semi-empirical model for correlating and predicting CO2 equilibrium solubility in aqueous 2-[2-(dimethylamino) ethoxy] ethanol solution. Separ. Purif. Technol., 124364